

Disk-Resident Graph ANN Search: An Experimental Evaluation

Xiaoyu Chen
Shanghai Jiao Tong
University
Chenxy1@sjtu.edu.cn

Jinxiu Qu
Shanghai Jiao Tong
University
afuloowa@sjtu.edu.cn

Yitong Song
Hong Kong Baptist
University
ytsong@hkbu.edu.hk

Shuhang Lu
Shanghai Jiao Tong
University
ts1989@sjtu.edu.cn

Huilong Li
Hong Kong Baptist
University
cshlli@comp.hkbu.edu.hk

Minghui Jiang
Shanghai Jiao Tong
University
tuanzi7@sjtu.edu.cn

Wei Zhou
Shanghai Jiao Tong
University
weizhoudb@sjtu.edu.cn

Jianliang Xu
Hong Kong Baptist
University
xujl@comp.hkbu.edu.hk

Xuanhe Zhou
Shanghai Jiao Tong
University
zhouxuanhe@sjtu.edu.cn

Fan Wu
Shanghai Jiao Tong
University
fwu@cs.sjtu.edu.cn

ABSTRACT

As data volumes grow while memory capacity remains limited, disk-resident graph-based approximate nearest neighbor (ANN) methods have become a practical alternative to memory-resident designs, shifting the bottleneck from computation to disk I/O. However, since their technical designs diverge widely across storage, layout, and execution paradigms, a systematic understanding of their fundamental performance trade-offs remains elusive.

This paper presents a comprehensive experimental study of disk-resident graph-based ANN methods. First, we decompose such systems into five key technical components, i.e., storage strategy, disk layout, cache management, query execution, and update mechanism, and build a unified taxonomy of existing designs across these components. Second, we conduct fine-grained evaluations of representative strategies for each technical component to analyze the trade-offs in throughput, recall, and resource utilization. Third, we perform comprehensive end-to-end experiments and parameter-sensitivity analyses to evaluate overall system performance under diverse configurations. Fourth, our study reveals several non-obvious findings: (1) vector dimensionality fundamentally reshapes component effectiveness, necessitating dimension-aware design; (2) existing layout strategies exhibit surprisingly low I/O utilization ($\leq 15\%$); (3) page size critically affects feasibility and efficiency, with smaller pages preferred when layouts are carefully optimized; and (4) update strategies present clear workload-dependent trade-offs between in-place and out-of-place designs. Based on these findings, we derive practical guidelines for system design and configuration, and outline promising directions for future research.

1 INTRODUCTION

Graph-based Approximate Nearest Neighbor (ANN) methods construct a proximity graph over high-dimensional vectors, where each vector connects to a set of approximate nearest neighbors. Queries are processed via best-first graph traversal, enabling an effective efficiency-accuracy trade-off. Owing to their strong empirical performance, graph-based approaches have become the state-of-the-art [18, 33] and are widely adopted in production systems such as Milvus [34], Elasticsearch [3], and PGVector [27].

Early graph-based ANN methods [5, 6, 21, 22, 26] are mainly designed to be memory-resident, with both raw vectors and graph structures stored entirely in memory. However, as data volumes

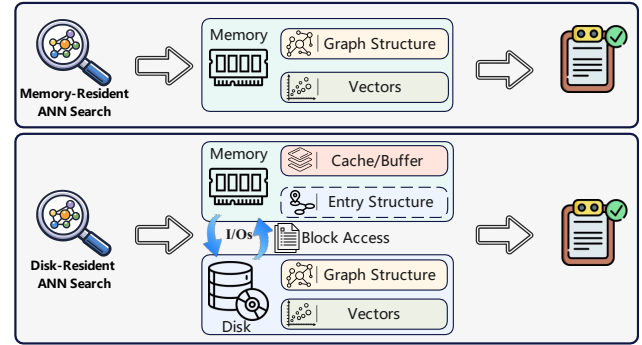


Figure 1: Memory-resident vs. disk-resident ANN search.

grow and memory remains expensive, this design becomes impractical, motivating a large body of disk-resident graph-based methods [8, 9, 13, 15, 16, 20, 25, 29, 32, 35, 38–40]. As shown in Figure 1, disk-resident designs differ fundamentally from memory-resident ones and several important factors should be carefully considered.

(1) Heterogeneous Storage and Layout. Disk-resident methods must determine how to place key data components, including raw vectors, graph index structures, and auxiliary data (e.g., entry structures and compressed vectors), across heterogeneous memory-disk storage. Different storage strategies directly determine both memory footprint and I/O volume, thereby exposing inherent trade-offs between query efficiency and memory usage [13, 32]. Moreover, since disk accesses are performed at block granularity, the physical layout of data within and across disk blocks plays a critical role in improving data locality and query performance [13, 15, 35, 38].

(2) Block-Level and Cache-Aware Query Processing. In disk-resident settings, ANN search no longer accesses individual vectors but entire disk blocks, leading to access patterns that differ fundamentally from memory-resident designs. As a result, the primary performance bottleneck shifts from in-memory computation to disk I/O, making I/O efficiency a key determinant of query performance. To mitigate disk access latency, existing methods incorporate (i) cache-aware techniques [15, 38, 40, 43], and (ii) asynchronous execution strategies [8, 15, 20, 35] during graph traversal, aiming to reduce both the number of I/O operations and the time spent waiting for I/O.

(3) Higher Update Overhead. Memory-resident graph-based ANN methods naturally support efficient insertions, as insertions can be applied directly to in-memory data structures. In contrast, in

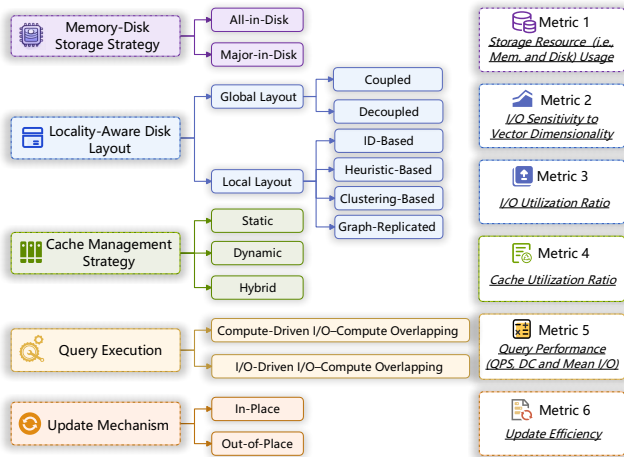


Figure 2: Technology decomposition and experimental study.

disk-resident settings, insertions can incur significantly high overhead, since a single insertion may require updating multiple related disk blocks. Moreover, deletions remain particularly challenging in disk-resident designs, as removing vectors can impair graph connectivity and consequently degrade query accuracy.

1.1 Our Motivation

(1) Lack of a Systematic Taxonomy and Comparison. Prior studies [2, 17, 36] have mainly focused on evaluating memory-resident graph-based ANN methods. By contrast, disk-resident approaches have undergone significant recent advancements, with substantially different architectural designs. Although a recent study [10] investigates I/O optimization along three design dimensions, it neither provides a unified taxonomy nor conducts a comprehensive comparative analysis of existing methods. Moreover, it overlooks critical factors such as data dimensionality and page size, and does not introduce dedicated metrics for fine-grained evaluation.

(2) Absence of a Unified Evaluation Framework. Existing methods are often evaluated in isolation or under method-specific configurations (e.g., fixed 16KB page sizes), which prevents fair and consistent comparisons. Therefore, a unified evaluation framework for systematically assessing their performance remains absent.

(3) Lack of Practical Design Guidelines. Disk-resident graph-based ANN systems consist of many interdependent components whose performance is jointly shaped by diverse data characteristics and system factors. However, practical guidelines for selecting appropriate design choices under varying data characteristics, system settings, and deployment constraints remain absent.

1.2 Our Contributions

Motivated by these observations, we present a comprehensive in-depth experimental study of disk-resident graph-based ANN search methods and make the following contributions.

(1) Technology Decomposition and Taxonomy (Section 3). As illustrated in Figure 2, we decompose existing methods into five core technique components: (i) memory-disk storage strategy, (ii) locality-aware disk layout, (iii) cache management strategy, (iv)

query execution, and (v) update mechanism. For each component, we further establish a structured taxonomy by categorizing existing approaches according to their underlying design principles, and define corresponding evaluation metrics to enable principled comparison across different methods.

(2) Fine-Grained Evaluation of Technique Components (Section 4.3). Leveraging carefully designed component-level metrics, we conduct controlled and fine-grained experiments on representative strategies within each technique component. We quantify their performance trade-offs, analyze sensitivity to key factors (e.g., dimensionality), and assess their impact on query efficiency.

(3) Overall End-to-End Performance Evaluation (Section 4.2). We further conduct comprehensive end-to-end evaluations under a unified and fair testbed. Our study includes a diverse set of representative systems (Table 1), each embodying different combinations of storage, layout, caching, asynchronous execution, and update strategies. We also systematically examine the impact of critical parameters (e.g., page size and beam width) on overall performance.

(4) Insightful Findings (Section 4). Based on our experimental results and in-depth analysis, we distill a set of insightful findings:

- ❶ PageANN excels at low dimensionality (i.e., d), whereas PipeANN dominates in high d . In high d , poor block locality makes multi-block accesses unavoidable, rendering asynchronous execution critical for hiding access latency. In contrast, at low d , stronger block locality makes disk layout more important for reducing accesses. These results highlight the need for *dimension-aware design choices*.
 - ❷ As d and required recall increase, the index-vector decoupled layout becomes increasingly advantageous over the widely used coupled layout. Moreover, overall I/O utilization remains consistently *low* across all layout strategies, typically below 15%.
 - ❸ Asynchronous execution masks computation costs, making I/O dominant in search latency. However, as d increases, computation overhead becomes more significant.
 - ❹ Lower d favors *dynamic/hybrid* caching, while higher d favors *static (graph-prioritized)* caching.
 - ❺ With small page sizes, carefully selecting high-quality neighbors is critical, whereas with larger page sizes, retaining more neighbors becomes advantageous.
 - ❻ Some methods become infeasible under small page sizes since a single page cannot accommodate their required data structures. When feasible, *smaller page sizes* generally yield higher efficiency.
 - ❼ In-place updates favor query-heavy workloads, whereas out-of-place updates better suit update-heavy or balanced workloads.
- (5) Usage Guidelines and Research Directions (Section 5).** We summarize practical guidelines for selecting and configuring disk-resident graph-based ANN techniques, and outline several promising directions for future research.

2 PRELIMINARIES

ANN Search. Given a vector dataset $\mathcal{D} = \{v_1, \dots, v_N\}$, a query vector q , and a similarity metric $sim(\cdot, \cdot)$ (e.g., Euclidean distance or cosine similarity), ANN search retrieves a set $S' \subseteq \mathcal{D}$ of k vectors that are approximately most similar to q . We focus on approximate search rather than exact search, as the latter is prohibitively expensive in high-dimensional spaces [6, 22]. By relaxing exactness, ANN achieves substantially higher query efficiency, with accuracy

Table 1: Comparison of Disk-Resident Graph-Based ANN Methods Across Key Design Dimensions.

Method	Storage Strategy	Layout Strategy		Cache Strategy	Asynchronous	Update Mechanism
		Global	Local			
DiskANN [13] / FreshDiskANN [29]	Major-in-Disk	Coupled	ID-Based	Static	✗	Out-of-Place
AiSAQ [32]	All-in-Disk	Coupled	ID-Based	✗	✗	✗
Starling [35]	Major-in-Disk	Coupled	Heuristic-Based	Static	Compute-Driven	✗
Gorgeous [38]	Major-in-Disk	Coupled	Graph-Replicated	Static	Compute-Driven	✗
PageANN [15]	All-in-Disk & Major-in-Disk	Coupled	Clustering-Based	Static	Compute-Driven	✗
PipeANN [8] / OdinANN [9]	Major-in-Disk	Coupled	ID-Based	✗	I/O-Driven	In-Place
DGAI [20]	Major-in-Disk	Decoupled	Clustering-Based	Hybrid	Compute-Driven	In-Place

✗ denotes not supported or not specified.

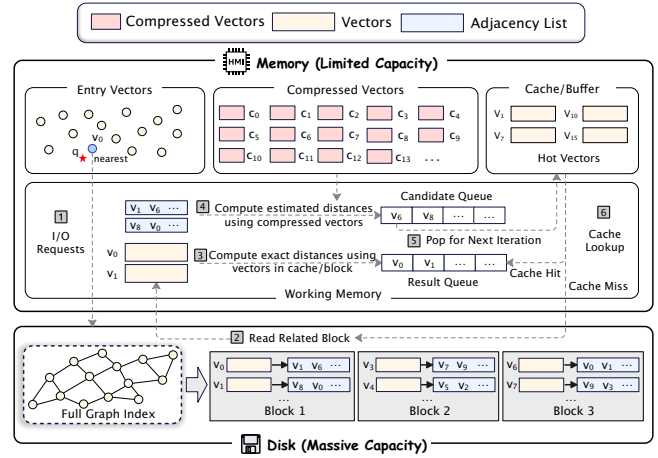
commonly measured by recall:

$$\text{Recall}@k = \frac{|S' \cap S|}{k},$$

where S denotes the exact k NN results. The goal of ANN search is to maximize recall (often $r \geq 0.9$) while minimizing query latency. **Disk-Resident Graph-Based ANN Search.** Graph-based methods [5, 6, 21, 22, 26, 41] are the state-of-the-art in ANN search, achieving an excellent trade-off between efficiency and accuracy [18, 33]. They organize vectors into an in-memory *proximity graph*, where each vector connects to a small set of approximate nearest neighbors, and answer queries via best-first graph traversal. However, as data volume grows, storing both high-dimensional vectors and graph adjacency structures entirely in memory becomes impractical. This has motivated a class of *disk-resident graph-based ANN* methods [8, 9, 13, 15, 16, 20, 25, 29, 30, 32, 35, 38–40, 42], which place memory-intensive components on disk while retaining lightweight structures in memory to preserve efficient traversal.

Figure 3 illustrates a representative disk-resident graph-based ANN workflow, as adopted by DiskANN [13]. The system partitions data structures into memory-resident and disk-resident components. In memory, three lightweight components are maintained: (1) *compressed vectors* (e.g., Product Quantization (PQ) codes [14]) for fast distance estimation, (2) *entry vectors* for traversal initialization, and (3) a *fixed-size buffer* that caches frequently accessed disk blocks. In contrast, storage-intensive data, including (1) full *graph adjacency lists* and (2) *raw vectors*, are stored on disk. To improve data locality, each disk block typically colocates a vector with its corresponding adjacency list.

During ANN search, the working memory maintains two intermediate priority queues: (1) a *candidate queue* that records unvisited candidate vectors ordered by their estimated distances, and (2) a *result queue* that maintains vectors with the smallest exact distances for final result construction. The search begins by identifying a nearest entry vector through entry vector scanning. The disk block containing the selected entry vector is then fetched, where exact distances to the query are computed to update the result queue, and estimated distances (via in-memory compressed vectors) of their neighbors are evaluated to update the candidate queue. Subsequently, the nearest unvisited vector is popped from the candidate queue, and the corresponding disk block is accessed. If the required vector is already cached in the in-memory buffer, the disk read is skipped. This process iterates until the smallest estimated distance

**Figure 3: Disk-resident graph-based ANN search.**

in the candidate queue exceeds the worst exact distance in the current result set, at which point further graph expansion cannot improve the top- k results. Finally, the top- k vectors in the result queue are returned as the ANN search results.

3 TECHNOLOGY ANALYSIS

The performance of disk-resident graph-based ANN search depends on multiple interacting design components that jointly affect query efficiency, recall, and system resource utilization. In this section, we decompose these components into several fundamental building blocks and analyze their respective roles and trade-offs.

(1) Memory-Disk Storage Strategy. Disk-resident ANN systems must determine how key data components, including compressed vectors, graph adjacency lists, and raw vectors, are partitioned between memory and disk. Different storage strategies directly affect query efficiency, memory footprint, and disk I/O volume, thereby inducing inherent trade-offs between query performance and resource utilization.

(2) Locality-Aware Disk Layout. Beyond deciding which components reside on disk, disk-resident ANN systems must also organize how disk-resident data are laid out. The physical layout directly affects data locality and I/O efficiency, thereby influencing query latency. Consequently, disk layout optimization has attracted significant research attention [15, 20, 24, 30, 35, 38, 39].

Table 2: Memory–disk storage strategies. *Legend:* ▶ = Compressed Entry Vectors, ▲ = Compressed Vectors, ■ = Sampled Entry Graph, ★ = Cache, ● = Adjacency Lists, and ◆ = Vectors.

Type	Method	Memory	Disk	Applications
Major-in-Disk★	DiskANN [13]	▲ ★	● ◆	(1) Low-latency/High-QPS ANN services. (2) Deployments with relatively sufficient memory budget.
	Starling [35]	▲ ■ ★	● ◆	
	Gorgeous [38]	▲ ■ ★	● ◆	
	MARGO [39]	▲ ■ ★	● ◆	
	BAMG [16]	▲ ■	● ◆	
	XN-Graph [40]	▲ ■	● ◆	
	DGAI [20]	▲ ★	● ◆	
	PipeANN [8]	▲ ■	● ◆	
All-in-Disk◊	PageANN [15]	▲ † ■ ★	▲ † ● ◆	(1) Memory-tight deployments (edge/on-device). (2) Scale-sensitive applications where dataset-scale ▲ cannot fit in memory.
	AiSAQ [32]	▶	▲ ● ◆	
	LM-DiskANN [25]	★	▲ ● ◆	
	LSM-VEC [42]	■ ★	● ◆	

★ **Major-in-Disk:** compressed vectors in memory; adjacency lists and vectors on disk.
 ◊ **All-in-Disk** (memory is still utilized): only auxiliary data in memory; all scale-growing components (i.e., compressed/raw vectors, and adjacency lists) on disk.

† Budget-dependent placement.

(3) **Cache Management Strategy.** Disk-resident ANN systems often rely on caching to reduce disk I/O by retaining frequently accessed data in memory during query processing. The effectiveness of caching depends on both *what* data are cached and *when* caching decisions are made, leading to different performance in terms of cache hit ratio and I/O reduction.

(4) **Query Execution.** Although most disk-resident graph-based ANN methods follow a similar graph traversal paradigm, execution-level optimizations play a critical role in query performance. In particular, asynchronous I/O and prefetching overlap disk access with computation, significantly affecting query latency. Different execution strategies expose trade-offs between query efficiency and system-level resource utilization.

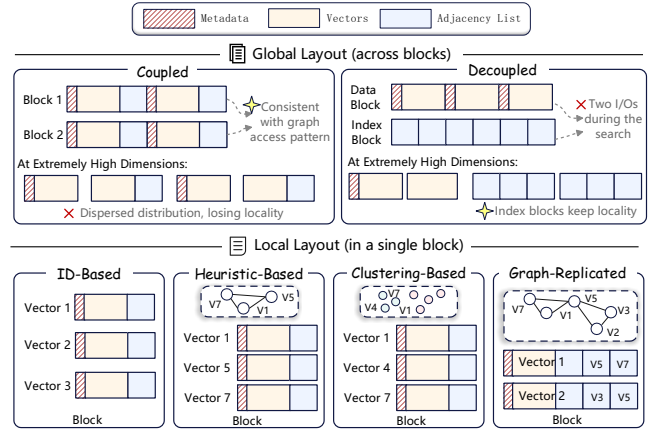
(5) **Update Mechanism.** To support dynamic workloads, disk-resident ANN systems adopt different update mechanisms [9, 29]. These mechanisms introduce distinct trade-offs among update efficiency, query performance, and maintenance overhead.

Building on this decomposition, we then systematically classify existing methods and analyze how different design choices affect query performance, resource utilization, and application suitability.

3.1 Memory-Disk Storage Strategy

Disk-resident graph-based ANN systems must carefully place three main components across memory and disk: (1) *compressed vectors* (typically PQ codes), (2) *graph adjacency lists*, and (3) *raw vectors*. These components scale linearly with data size, whereas other structures, such as entry vectors/graph and caches, incur only bounded overhead. Based on whether scale-growing data is stored in memory, existing designs can be broadly classified into *major-in-disk* and *all-in-disk* strategies. Table 2 summarizes representative methods under these two categories.

Major-in-Disk. Major-in-disk is the most widely adopted storage strategy [8, 13, 16, 20, 35, 38–40], where compressed vectors reside in memory and graph adjacency lists together with raw vectors are stored on disk. The key insight is that compressed representations are lightweight yet frequently accessed during graph traversal for


Figure 4: Locality-aware disk layout strategies.

neighbor distance estimation, making them well suited for memory residency. As a result, major-in-disk designs enable faster candidate scoring and prioritization with fewer disk accesses, substantially reducing disk I/O during search. However, this benefit comes at the cost of memory footprints that grow linearly with data scale and may become prohibitive under strict memory budgets.

All-in-Disk. All-in-disk methods [15, 25, 32, 42] place all scale-growing components on disk, keeping only a small and controllable set of auxiliary structures (e.g., entries and caches) in memory. This design minimizes memory footprint and makes all-in-disk designs particularly suitable for memory-constrained environments. To reduce redundant disk accesses, these methods often co-locate compressed vectors (e.g., PQ codes) with graph adjacency lists so that traversal signals and approximate distance estimates can be obtained from a single disk fetch. However, since both traversal and scoring information are disk-resident, this design typically incurs more disk I/Os along the search path, which can degrade throughput and tail latency.

► **Evaluation Preview.** In Section 4.3.1, we quantify the memory and disk footprints of both strategies and identify the memory threshold beyond which the major-in-disk design becomes infeasible and must fall back to an all-in-disk placement.

3.2 Locality-Aware Disk Layout

Careful layout of adjacency lists and raw vectors within disk blocks to improve data locality is critical for minimizing I/O cost. As shown in Figure 4, layout decisions can be characterized at two levels: *global* and *local*. Global layout determines how adjacency lists and raw vectors are distributed across disk blocks, while the local layout specifies how these components are organized within each block.

3.2.1 Global Layout. Based on whether adjacency lists and raw vectors are co-located within the same disk blocks, existing global layouts can be classified into *coupled* and *decoupled* designs.

Coupled Layout. As illustrated in Figure 4, the coupled layout colocates each raw vector (and its metadata) with its adjacency list within the same disk block, which is widely adopted by several methods, including DiskANN [13], Starling [35], and PageANN [15]. This layout aligns well with graph-based ANN traversal, where result evaluation and neighbor expansion are performed together,

making tight colocation natural for the access pattern. However, at very high dimensionality (e.g., ≥ 1000), a disk block may hold only a single raw vector, leading to fragmented placement and degraded data locality, which ultimately limits I/O efficiency.

Decoupled Layout. The decoupled layout stores adjacency lists and raw vectors separately in index blocks and data blocks, respectively, which is adopted by recent methods such as DGAI [20], TRIM [30], BAMG [16], and GaussDB-Vector [31]. While decoupling adjacency lists from raw vectors risks doubling the I/O per traversal step, this penalty is mitigated by pruning strategies that bypass unnecessary data block accesses [20, 30]. At high dimensionality, this layout achieves better locality: short adjacency lists allow many graph entries to be packed into a single index block, while pruning skips most data blocks, substantially reducing overall I/O cost.

► **Evaluation Preview.** The above analysis indicates that data dimensionality plays a critical role in determining an appropriate global layout. In Section 4.3.2, we evaluate the impact of data dimensionality on global layout choices and derive practical guidelines for selecting an appropriate global layout under different dimensionality regimes.

3.2.2 Local Layout. Local layout determines which vectors and their adjacency lists are colocated within the same disk block (under the coupled global layout), when a disk block can accommodate multiple data items as determined by the *page size*. By improving data locality, an effective local layout enhances I/O utilization and reduces overall I/O cost. As illustrated in Figure 4, existing local layout strategies can be broadly classified into four categories: *ID-based* [8, 13, 25, 32], *heuristic-based* [35, 39], *clustering-based* [15, 20, 43], and *graph-replicated* [38].

ID-Based. The ID-based layout organizes vector items within disk blocks based on their data identifiers, which is initially adopted by DiskANN [13]. This simple layout incurs no extra computational overhead, but it is largely oblivious to the graph search pattern. Vectors with consecutive IDs are not necessarily close in the graph, nor are they frequently accessed together during graph traversal.

Heuristic-Based. Heuristic-based layouts explicitly exploit graph topology and aim to colocate neighboring vectors within the same disk block to improve data locality. Prior work [35] shows that optimally serializing a graph into disk blocks while minimizing cross-block accesses is an NP-hard problem. As a result, they mainly rely on heuristics that incrementally place a vector into the disk block containing the largest number of its already-placed neighbors. Albeit without optimality guarantees, heuristic-based layouts can achieve better I/O utilization and reduced I/O cost in practice.

Clustering-Based. Clustering-based layouts group vectors belonging to the same cluster into the same disk block, prioritizing vector similarity over graph topology. This design is motivated by the observation that long graph edges are often introduced to maintain connectivity or search diversity and thus do not necessarily reflect proximity in the original vector space [43]. By collocating similar vectors, clustering-based layouts improve spatial locality and reduce I/O cost during ANN search.

Graph-Replicated. Graph-replicated layout stores multiple adjacency lists together with a single raw vector in the disk block, motivated by the fact that adjacency lists are accessed far more

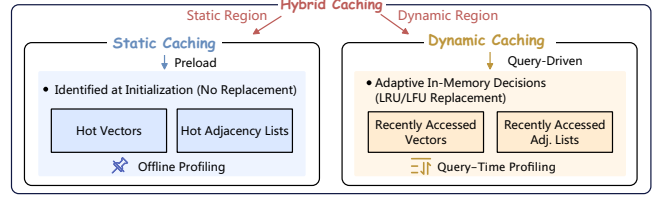


Figure 5: Cache strategies.

frequently than raw vectors during graph traversal [38]. As illustrated in Figure 4, a graph-replicated block not only stores a raw vector (e.g., v_1) together with its own adjacency list, but also includes the adjacency lists of its neighboring vectors (e.g., v_5 and v_7). By duplicating neighbor information, this design reduces random I/O incurred by repeatedly fetching adjacency lists, at the cost of additional storage overhead due to replication.

► **Evaluation Preview.** In Section 4.3.2, we evaluate the four classes of local layouts with a focus on their I/O utilization. Specifically, we quantify how much of the raw vectors and adjacency lists read from disk are actually useful for graph traversal. In addition, since *page_size* is a key factor affecting data locality and query efficiency, we examine its impact separately in Section 4.2.3.

3.3 Cache Management Strategy

Caches are commonly employed in disk-resident ANN search to keep frequently accessed or potentially useful data in memory, thereby reducing disk I/O. As shown in Figure 5, we classify existing cache management strategies into three categories: static [13, 15, 35, 38], dynamic [40], and hybrid caching strategies [20, 43].

Static Caching. Static caching pre-identifies frequently accessed data, commonly referred to as *hot* data, and retains them in memory. Such hot items typically originate from hub vectors that play a critical role in graph navigation, or from answer vectors corresponding to popular or recurring query topics. By caching such hot items, static caching can significantly improve query throughput, as most vectors are rarely accessed in practice [11, 12]. However, this strategy is sensitive to workload skew and may incur high query latency for cold or previously unseen queries whose access patterns deviate from the cached hot set.

Dynamic Caching. Dynamic caching adaptively maintains raw vectors and adjacency lists in memory based on runtime access patterns. Using online replacement policies (e.g., LRU or LFU), it captures temporal locality and accommodates evolving workloads, effectively reducing latency for changing or unseen queries. However, dynamic cache maintenance introduces additional computational overhead, and its effectiveness diminishes when access patterns are highly random.

Hybrid Caching. Hybrid caching combines static and dynamic caching by partitioning memory into a static region for long-term hot items and a dynamic region managed by online replacement policies to capture transient access patterns. This design balances throughput and latency across diverse query workloads, but its effectiveness depends on proper memory partitioning and tuning.

► **Evaluation Preview.** In Section 4.3.3, we conduct a comparison of the three cache management strategies, examining which design achieves higher cache utilization.

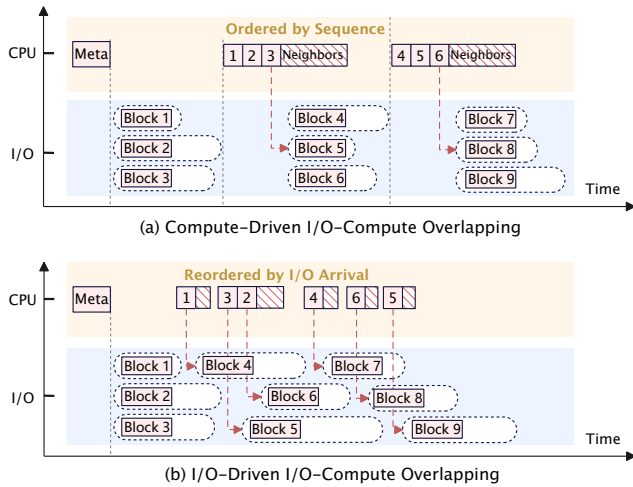


Figure 6: Compute-Driven vs. I/O-Driven Overlapping

3.4 Query Execution

Query execution in disk-resident graph-based ANN search largely follows a standard best-first graph traversal process, as described in Section 2. In this workflow, memory-resident compressed vectors are typically used for distance estimation, while disk-resident adjacency lists and full-precision vectors are accessed for candidate expansion and result evaluation. Depending on the adopted storage, layout, and caching strategies, existing methods introduce targeted modifications to this baseline procedure. For example, *all-in-disk* designs perform distance estimation using disk-resident compressed vectors [15, 25, 32], *decoupled layouts* separate navigation and refinement with additional pruning to reduce data accesses [20, 30], and *dynamic caching* adaptively determines which vectors and adjacency lists to retain in memory at runtime [20, 40, 43].

To mitigate high latency of disk accesses, modern systems widely adopt asynchronous execution to overlap I/O operations with CPU computation, reducing I/O stall time. Depending on whether subsequent I/O requests are determined by intermediate computation results or issued speculatively and filtered by later computation, existing I/O-compute overlap strategies can be broadly classified into two categories: *compute-driven* [15, 35, 38] and *I/O-driven* [8]. **Compute-Driven I/O-Compute Overlapping.** As shown in Figure 6(a), compute-driven overlapping follows a strictly computation-determined execution order. After reading metadata, the CPU processes candidate vectors sequentially within a beam of limited width, and issues the next I/O request only after intermediate computation determines which data blocks are required. As a result, disk I/O requests are tightly coupled with computation results, and blocks are fetched on demand in a well-defined sequence. This design aligns well with graph traversal patterns and avoids unnecessary disk reads. However, since I/O requests are generated only after computation completes for the current beam, the degree of I/O-compute overlap is limited, potentially leaving available I/O bandwidth underutilized.

I/O-Driven I/O-Compute Overlapping. In contrast, Figure 6(b) illustrates an I/O-driven overlapping strategy, where disk I/O is

issued speculatively and decoupled from the exact computation order. After metadata access, the system proactively submits multiple I/O requests for candidate blocks, typically determined by a beam width that controls the number of prefetched candidates. As disk blocks return asynchronously, the CPU processes available data immediately and reorders computation according to I/O arrival order rather than traversal sequence. This approach maximizes I/O-compute overlap and improves I/O bandwidth utilization, but may incur redundant disk reads and additional memory pressure due to speculative prefetching.

► **Evaluation Preview.** In Section 4.2, we evaluate the end-to-end query performance of representative disk-resident graph-based methods, covering a range of storage, layout, and caching strategies, and analyze their sensitivity to the parameter *beam_width*. To further examine CPU and I/O efficiency, Section 4.3.4 provides a detailed breakdown of query execution costs, using the number of distance computations to measure CPU overhead and the number of disk I/O operations to characterize I/O performance.

3.5 Update Mechanism

Under dynamic workloads, disk-resident graph-based ANN methods support continuous insertions and deletions while targeting three goals: (1) preserving graph connectivity, (2) maintaining query efficiency, and (3) minimizing update overhead. Based on when updates are materialized, existing methods can be classified into *in-place* [9, 20, 25, 27, 31] and *out-of-place* [23, 29, 34, 37, 42] updates. **In-Place Update.** In-place designs apply modifications directly to the disk-resident graph as updates arrive. A typical in-place mechanism is to edit on-disk adjacency immediately and perform local graph topology maintenance (e.g., linking, pruning, and reconnection) so that the graph remains searchable right after each update [20, 25]. Another in-place variant still writes updates to disk on the critical path, but avoids doing *all* cleanup work synchronously: deletions may be recorded in-place while space reclamation and structural tidying are deferred to maintenance, without introducing a separate memory-resident delta that must later be merged into the main index [9, 27, 31]. This strategy provides strong freshness and avoids a multi-component index state, but its cost is sensitive to random I/O and write interference, as a single update may touch multiple pages and contend with foreground search.

Out-of-Place Update. Out-of-place designs first accumulate modifications in memory and then write them to disk in a batched manner. A representative implementation is an LSM-style consolidation pipeline, where updates are absorbed into memory and periodically merged/compacted into a disk-resident graph index [23, 29, 34, 42]. Another implementation maintains a memory-resident overlay that is immediately visible to queries and asynchronously integrated into the base graph index, so that updates become searchable without immediately rewriting the disk graph [37]. This strategy improves write throughput by amortizing many small changes into batched disk writes and better isolating reads from writes, but it introduces a multi-component index state and costly background consolidation.

► **Evaluation Preview.** In Section 4.3.5, we evaluate in-place and out-of-place update strategies, comparing their average update latency and analyzing how query performance evolves as updates accumulate over time.

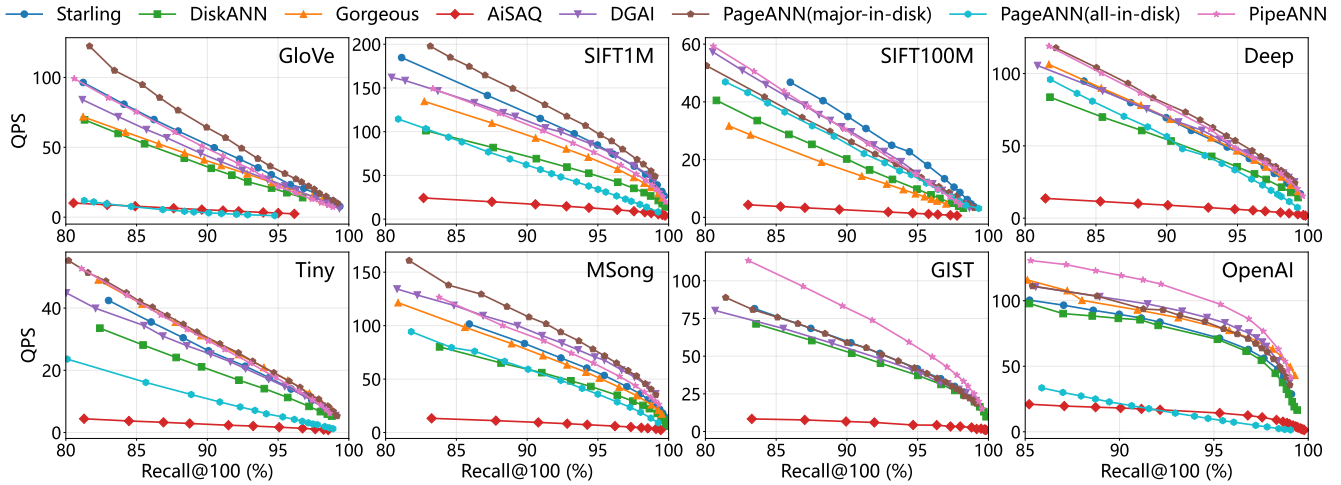


Figure 7: QPS vs. recall across all datasets.

4 EXPERIMENTS

4.1 Experimental Setup

Datasets. As summarized in Table 3, we evaluate our methods on eight benchmark vector datasets [1, 7, 28] spanning diverse scales, dimensionalities, and data sources. End-to-end QPS and recall are evaluated on all datasets, while other experiments are primarily conducted on the SIFT, Deep, and GIST datasets. Moreover, the OpenAI dataset with 3,072 dimensions is used to study the impact of increasing dimensionality on different global layouts.

Table 3: Datasets statistics and parameter settings. *R*: maximum degree; *Samp.*: in-memory navigation graph sampling rate; *Cache*: static cache budget (as a fraction of dataset size); *Page*: page size; *PQ m*: number of PQ subspaces.

Dataset	Dataset Statistics				Parameter Settings					
	Dim	Type	#Vectors	#Queries	Src	<i>R</i>	<i>Samp.</i>	<i>Cache</i>	<i>Page</i>	<i>PQ m</i>
GloVe	100	float	1,183,514	1,000	Text	48	0.5%	1%	4KB	25
SIFT1M	128	float	1,000,000	10,000	Image	48	0.5%	1%	4KB	16
SIFT100M	128	uint8	100,000,000	10,000	Image	48	0.5%	1%	4KB	16
Deep	256	float	1,000,000	1,000	Image	48	0.5%	1%	4KB	32
Tiny	384	float	5,000,000	1,000	Image	48	0.5%	1%	4KB	48
MSong	420	float	992,272	1,000	Audio	48	0.5%	1%	4KB	64
GIST	960	float	1,000,000	1,000	Image	48	0.5%	1%	4KB	120
OpenAI	3,072	float	1,000,000	1,000	Text	48	0.5%	1%	16KB	384

Compared Methods. As shown in Table 1, we select seven representative open-source disk-resident graph-based ANN methods for evaluation, spanning a broad design space in terms of storage placement, disk layout, caching strategies, query execution models, and update mechanisms. Specifically, the evaluated methods include DiskANN [13] and its update-enhanced variant FreshDiskANN [29], AiSAQ [32], Starling [35], Gorgeous [38], PageANN [15], PipeANN [8] and its update-enhanced variant OdinANN [9], and DGAI [20].

Implementations. We implement the compared methods in C++ (GCC -O3). The experimental platform is a Linux server powered by dual Intel Xeon Platinum 8457C processors (96 cores, 512 GB RAM), vector data and indexes are placed on a 1.92TB Samsung Enterprise SSD. During search, we use a single thread, while for dynamic scenarios, update efficiency is evaluated using 9 threads for insertions and 1 for deletions, concurrent with 16 search threads.

4.2 End-to-End Evaluation

4.2.1 Trade-offs between QPS and Recall. Figure 7 compares end-to-end query performance across eight benchmark vector datasets. PageANN (major-in-disk) excels in low-to-medium dimensions at small to medium scales, while PipeANN dominates high-dimensional GIST and OpenAI. At 0.95 recall, PageANN (major-in-disk) dominates most low-to-medium dimensions (<420), outperforming PipeANN by 42.8% on GloVe, 25.7% on SIFT1M, 10.5% on Deep, 8.5% on Tiny, and 20.1% on MSong. This trend shifts on SIFT100M, where Starling surpasses PageANN by 43.7%. In high dimensions, PipeANN surpasses PageANN by 40.5% on GIST and 15.6% on OpenAI. PageANN’s advantage in low dimensions stems from a lightweight in-memory hash table for efficient entry selection and a block-aligned graph index that maximizes useful data per I/O. As dimensionality grows, PipeANN’s I/O-compute overlapping reduces latency from multiple block accesses. On SIFT100M, PageANN(major-in-disk) performance drops due to neighbor-pruning that lowers intra-page out-degree, while all-in-disk and major-in-disk variants show similar performance by preserving comparable connectivity.

Across benchmarks, major-in-disk designs consistently outperform all-in-disk variants. For GloVe and GIST, a 3.1×–7.6× memory overhead yields 10.7×–13.7× QPS gains. For Tiny and OpenAI, speedups reach 3.8×–6.8× with 10.5×–15.6× memory overhead. On SIFT1M, Deep, and MSong, they deliver 1.6×–2.5× speedups with 2.1×–3.0× more memory. Only on SIFT100M are gains limited to 1.8× despite 149.8× more memory.

Findings: (1) PageANN (major-in-disk) outperforms in low dimensions, whereas PipeANN dominates in high dimensions, underscoring the need for *dimension-aware design choices*. In high-dimensional settings, poor block locality makes multi-block accesses inevitable, favoring I/O-driven overlapping to hide read latency. In contrast, at lower dimensions, stronger block locality makes graph topology and layout more critical for reducing block accesses. (2) *Major-in-disk* designs deliver a 1.6×–13.7× improvement than *all-in-disk*, highlighting the effectiveness of keeping compressed vectors in memory.

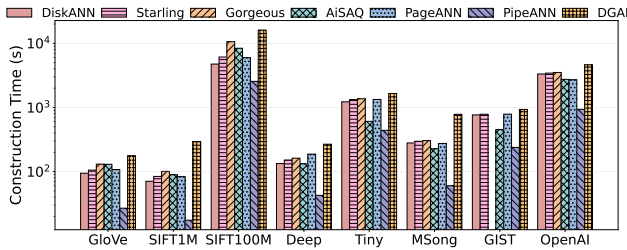


Figure 8: Index construction time.

4.2.2 Index Construction Time. Figure 8 shows the index construction time of seven algorithms across eight datasets. Overall, PipeANN consistently achieves the shortest index construction time across all datasets. This advantage is particularly pronounced on the high-dimensional OpenAI dataset, where PipeANN achieves a speedup of approximately 2.9 \times over AiSAQ and PageANN, while outperforming DiskANN, Starling, and Gorgeous by 3.5 \times , 3.6 \times , and 3.7 \times , respectively. Compared to DGAI, it reaches a maximum efficiency gain of nearly 5.0 \times . PipeANN’s construction efficiency mainly comes from PQ training with Elkan [4], instead of the distance-exhaustive Lloyd’s algorithm [19] used by most methods. By leveraging the triangle inequality, Elkan pruning can significantly reduce redundant distance calculations and accelerate clustering.

Findings: The Elkan algorithm [4] enables more efficient PQ training than widely used Lloyd’s algorithm [19] when sufficient memory is available.

4.2.3 Impact of Page Size. Figure 9 shows the impact of page size on query efficiency. For most methods, QPS drops as page size increases. While QPS generally declines as page size increases from 4 KB to 16 KB, Starling exhibits a counterintuitive improvement at 16 KB. On SIFT1M: At 4 KB and 8 KB, PageANN (major-in-disk) performs best, outperforming the runner-up by 11.2%–25.8% and 5%–9% at equal recall. At 16 KB, Starling ranks first, surpassing runner-up by 2.8%–28%. At small page sizes, PageANN benefits from clustering-based layout with node contraction and neighbor pruning. As page size grows, the capped neighbor limit reduces the average out-degree and weakens connectivity. In contrast, Starling uses heuristic-based layout without a strict neighbor cap, preserving richer connectivity and outperforming PageANN. Detailed comparisons are provided in Section 4.3.2.

It’s important to note that not all algorithms maintain stability across page sizes. For instance, on GIST with 4 KB pages, Gorgeous fails to construct the graph index with $R = 48$, while PageANN (all-in-disk) becomes highly inefficient because limited block space reduces the neighbor pruning threshold to 2.

Findings: (1) PageANN (major-in-disk) performs best under small page sizes (4KB/8KB), while Starling dominates at 16KB. This suggests that with small page sizes, selecting high-quality neighbors is critical, whereas with larger page sizes, retaining more neighbors becomes advantageous. (2) Some methods become infeasible under small page sizes since a single page cannot accommodate their required data structures. When feasible, *smaller page sizes* generally yield higher efficiency.

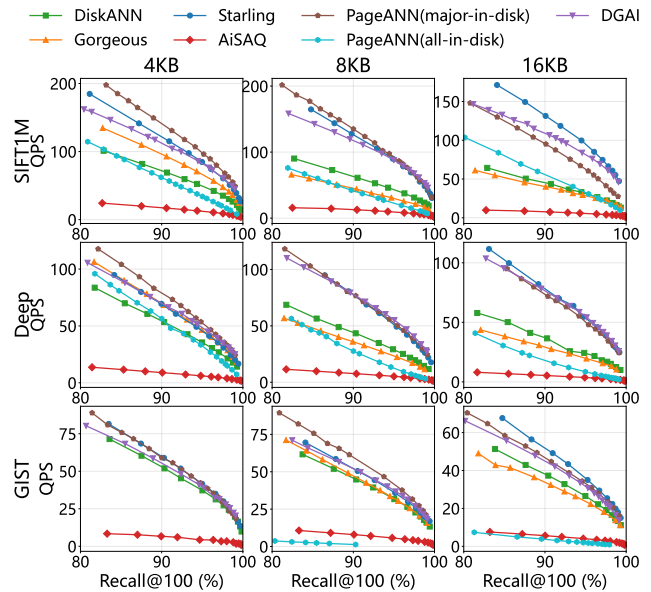


Figure 9: QPS vs. recall for different page sizes.

4.2.4 Impact of Beam Width. Figure 10 shows the impact of varying the beam width (W) on query efficiency across different datasets and recall targets. Overall, the QPS of almost all methods increases as beam width grows. The most substantial gains occur between $W = 1$ and $W = 8$. For SIFT1M at 0.95 recall, increasing W from 1 to 4 yields a QPS improvement of approximately 2.8 \times to 3.4 \times for methods like DiskANN and PipeANN. When W further increases from 4 to 8, the QPS still exhibits a substantial growth of approximately 45% to 75%. However, marginal gains diminish significantly beyond $W = 16$. Despite doubling the width from 16 to 32, QPS growth for most algorithms (e.g., Starling and Gorgeous) typically drops below 15% or even plateaus. This exposes a fundamental system trade-off: while a wider beam width initially improves throughput via I/O batching, these gains are eventually bottlenecked by SSD concurrency limits and offset by the computational overhead of managing a larger candidate pool.

Findings: Increasing the beam width improves query performance, but the marginal gains progressively diminish, plateauing at around 16 in our settings.

4.3 Fine-Grained Evaluation

4.3.1 Storage Strategy Evaluation. Table 4 details the disk (GB) and memory (MB) footprints of different disk-resident graph-based ANN methods, which are classified into major-in-disk and all-in-disk strategies, across eight benchmark datasets.

Regarding memory overhead, major-in-disk configurations demand a significantly larger portion of memory, while all-in-disk strategies maintain a minimal and strictly constant footprint between 25.5 MB and 48 MB regardless of the dataset. Specifically, major-in-disk strategies’ memory footprints account for 22.59%–35.44% of the raw data size on GloVe, 12.60%–25.60% on SIFT1M, 18.21%–39.46% on SIFT100M, 9.06%–20.28% on Deep, 4.08%–8.87%

Table 4: Disk (GB) and Memory (MB) Usage Across Datasets (Min/Max highlighted *per dataset* across all methods).

Type	Method	GloVe		SIFT-1M		SIFT-100M		Deep		Tiny		MSong		GIST		OpenAI	
		Disk	Mem	Disk	Mem	Disk	Mem	Disk	Mem	Disk	Mem	Disk	Mem	Disk	Mem	Disk	Mem
Major-in-Disk	DiskANN	0.790	160	0.811	108	31.908	2859	1.368	175	9.681	530	2.052	279	4.174	574	16.399	933
	Starling	0.790	123	0.811	120	31.908	3819	1.368	196	9.681	595	2.052	306	4.174	628	16.399	1039
	Gorgeous	5.493	138	4.768	109	413.259	3056	5.277	198	29.564	445	5.878	193	-	-	30.708	818
	PipeANN	0.752	153	0.763	125	31.789	2547	1.272	155	9.537	430	1.896	194	3.815	274	15.259	749.5
	DGAI	0.693	114	0.684	82	30.990	4817	1.144	124	10.494	650	2.090	201	4.001	366	16.230	1018
	PageANN [†]	0.613	102	0.605	61.5	21.202	2223	1.367	88.5	9.684	298.5	2.053	100.5	4.186	169.5	16.529	456
All-in-Disk	AiSAQ	1.570	33	1.335	30	54.496	28.5	2.033	31.5	9.905	33	2.118	31.5	4.286	36	16.408	48
	PageANN [‡]	0.514	43.5	0.558	30	63.580	25.5	1.270	30	9.540	28.5	1.900	34.5	-	-	15.260	45

Notes: blue = minimum, red = maximum within each dataset and metric (Disk or Mem) across all methods; ties are highlighted; missing entries (-) are excluded.

[†] PageANN major-in-disk version.

[‡] PageANN all-in-disk (low-memory) version.

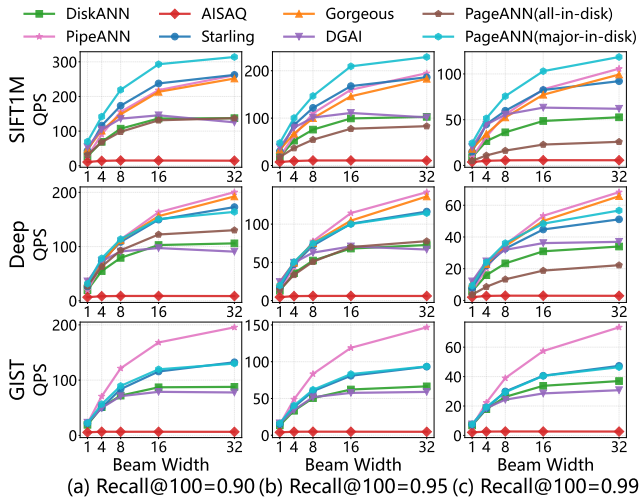


Figure 10: QPS vs. recall for different beam widths.

on Tiny, 6.32%–19.25% on MSong, 4.63%–17.15% on GIST, and 3.89%–8.87% on OpenAI. Among these, Starling typically dominates memory consumption on high-dimensional datasets, peaking at 628 MB on GIST and 1039 MB on OpenAI. This high memory requirement is necessary because major-in-disk strategies must maintain massive auxiliary structures in memory—such as PQ Codes, cached graph nodes, and a navigation index.

Regarding disk usage, Gorgeous consistently requires the most storage, reaching 413.259 GB on SIFT100M and 30.708 GB on OpenAI, because of its separate adjacency and vector files for its cache strategy along with redundant neighbor storage within disk blocks. On the other end of the spectrum, by avoiding duplicate neighbor storage and applying neighbor pruning, PageANN (all-in-disk) achieves a more compact index with higher storage utilization, with a minimum of 0.514 GB on GloVe and 0.558 GB on SIFT1M. In high-dimensional settings, PipeANN exhibits the lowest disk usage among all methods, such as 15.259 GB on the 3,072-dimensional OpenAI dataset, primarily because it incurs less overhead from auxiliary files required for search.

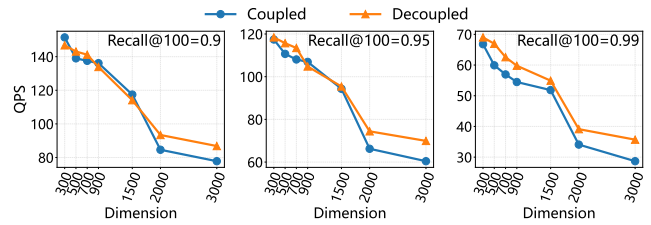


Figure 11: QPS vs. dimension for different global layouts.

Findings: (1) Major-in-disk designs usually incur 3.4×–18.0× higher memory cost than all-in-disk designs while reaching 143.1× on SIFT100M. (2) In low dimensions, disk usage is primarily determined by disk layout and graph structure. In high dimensions, it is dominated by raw vector size, resulting in similar usage across different methods.

4.3.2 Layout Strategy Evaluation. We evaluate global and local layout strategies separately to understand their individual impact on I/O behavior and query performance.

Global Layout Evaluation. Figure 11 shows the query efficiency (QPS) of two global layout strategies on OpenAI across various dimensions and recall targets. Overall, query efficiency for both strategies declines as dimensionality increases. Coupled layout performs better in low dimensions, while decoupled layout proves more effective as dimensionality and recall targets scale. At 3000 dimensions, decoupled layout outperforms the coupled one by 13.05%, 15.74%, and 24.44% at recall targets of 0.90, 0.95, and 0.99. Furthermore, while QPS decreases marginally as dimensionality grows from 500 to 900 (fixed 4KB page), it plummets when scaling from 900 to 1500 as page size expands to 8KB. For instance, at 0.9 recall, both layouts show slight QPS declines (2.05% and 6.43%) from 500 to 700, but drop sharply by about 14.5% from 900 to 1500.

Meanwhile, under a fixed page size, different block allocation strategies in coupled and decoupled layouts cause block utilization variance and noticeable performance fluctuations. For instance, at 0.9 recall, 4KB page size, and 500 dimensions, a coupled-layout block fits only one node (53.61% block utilization), whereas the decoupled layout fits two (97.66%). Consequently, the search efficiency of the

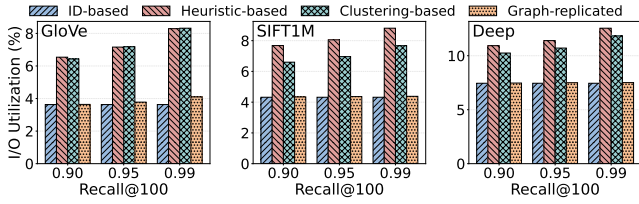


Figure 12: I/O utilization of local layouts (16KB page size).

decoupled layout slightly surpasses that of the coupled layout at this specific lower dimensionality (dimension=500).

Findings: (1) As dimensionality and recall increase, decoupled layouts become more advantageous by managing vectors and the graph index separately and effectively reducing vector reads (with a crossover around 1,500D). (2) Higher dimensionality often necessitates larger page sizes, causing QPS to decline in discrete steps rather than smoothly. (3) Even under the same dimensionality and page size, different global layouts lead to varying block utilization, affecting query performance.

Local Layout Evaluation. To investigate the effectiveness of block layout, we measure the I/O utilization, defined as the ratio of total data size required by the search path to the total data volume read under a fixed page size of 16KB. Figure 12 shows the I/O utilization of four local layout strategies across different datasets and recall targets. Overall, heuristic-based layout achieves the highest I/O utilization in most cases, followed by clustering-based approach. On average across the three datasets, heuristic-based layout outperforms ID-based, clustering-based and graph-replicated layouts by 1.91 \times , 1.16 \times , and 1.83 \times , respectively. Furthermore, as accuracy increases, the heuristic-based strategy demonstrates a more significant efficiency growth than others. For instance, on GloVe dataset, the performance gap between heuristic-based layout and ID-based baseline widens from 1.80 \times at 0.9 recall to 2.28 \times at 0.99 recall. However, despite these improvements, the overall utilization remains remarkably low. Across all datasets and strategies, the peak I/O utilization achieved by heuristic-based layout on Deep dataset reaches only 12.55%, which remains well below 15%. This indicates that a vast majority of the data loaded during each I/O operation remains unused, leaving significant room for optimization.

Findings: (1) Overall I/O utilization remains *low* across all methods, not exceeding 15%. (2) Heuristic-based layouts achieve higher I/O utilization by leveraging graph topology.

4.3.3 Cache Strategy Evaluation. We evaluate caching effectiveness using the per-hop cache hit rate, which represents the percentage of cache-served accesses during the search process. Figure 13 compares the cache hit rates of four strategies across different datasets as the search progresses through hops. Overall, dynamic and hybrid strategies exhibit superior performance on low-dimensional datasets, while static (graph-prioritized) strategy demonstrates greater robustness on high-dimensional data. Specifically, dynamic and hybrid strategies outperform static (graph-prioritized) baseline by 2.75 \times and 2.60 \times on SIFT1M dataset, and 1.24 \times and 1.08 \times on Deep dataset. Furthermore, they exceed static (hot data) strategy by up

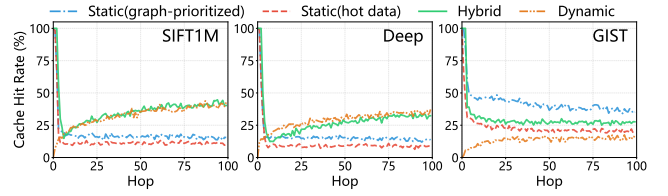


Figure 13: Cache hit rate vs. search hops.

to 4.69 \times on Deep dataset. However, this trend reverses on the high-dimensional GIST dataset, where static (graph-prioritized) strategy achieves a hit rate 2.22 \times higher than dynamic baseline, which drops to 15.82%. This performance shift is driven by the impact of vector dimensionality on block utilization. In low-dimensional settings, allowing dynamic/hybrid strategies to fetch more useful information per I/O. As dimensionality increases, the number of vectors per block decreases sharply, diminishing the gains of dynamic loading. Conversely, by prioritizing compact adjacency lists over bulky vectors, static (graph-prioritized) strategy covers a broader graph topology under a fixed memory budget of 1% size of datasets, maintaining superior hit rates during long-tail search paths.

Findings: The optimal caching strategy depends on dimensionality: *dynamic* and *hybrid* caching perform best in low dimensions, whereas *static (graph-prioritized)* is more effective in high dimensions.

4.3.4 Query Strategy Evaluation. Figures 14 (a)-(c) illustrate the mean I/Os, average distance computations, and the breakdown of time consumed by I/Os versus other stages under varying search queue length (L). All-in-disk methods are excluded due to their non-comparable I/O scales. The overall observations are as follows: (1) Average I/Os among major-in-disk algorithms: DGAI exhibits the highest I/O frequency, while PageANN achieves the lowest. On SIFT1M, DGAI requires 1.58 \times to 1.73 \times more I/Os than PageANN, attributed to its decoupled layout that necessitates separate I/O requests for retrieving topological and vector information and poor pruning of inaccurate PQ. (2) Regarding Average Computations: PageANN reports the highest computational time overhead across all datasets, whereas PipeANN maintains the lowest. On SIFT1M, PageANN’s computation time is 2.75 \times to 2.92 \times that of PipeANN. This is because PageANN executes extensive PQ-based distance calculations for entry-point selection via hash tables. Furthermore, exact distance evaluation contributes only 10.07% to 37.38% of the total computation time, remaining substantially smaller than the PQ time cost (3)I/O and Computation Time: It is noteworthy that disk I/O time dominates the overall execution, accounting for 80% to 99.6% of the total query time. This confirms that disk I/O overhead has become the primary bottleneck limiting search performance.

Findings: (1) I/O-driven overlapping incurs no additional I/O under a consistent layout (i.e., DiskANN and PipeANN) in a single-threaded setting. (2) Optimized layouts (e.g., Starling and PageANN) substantially reduce I/O accesses. (3) Asynchronous execution masks computation costs, making I/O dominant in search latency. However, as dimensionality increases, computation overhead becomes more significant.

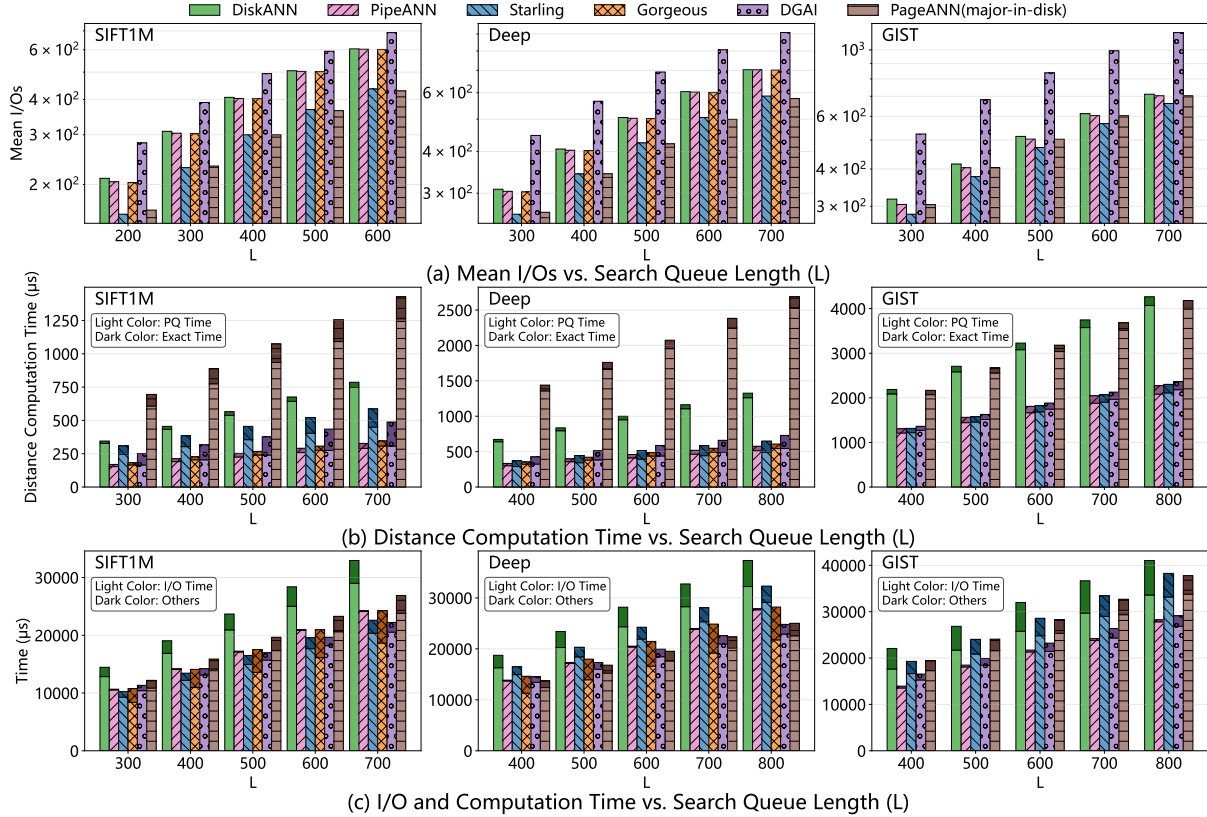


Figure 14: Comparison of mean I/Os, computational overhead, and time decomposition for different search strategies.

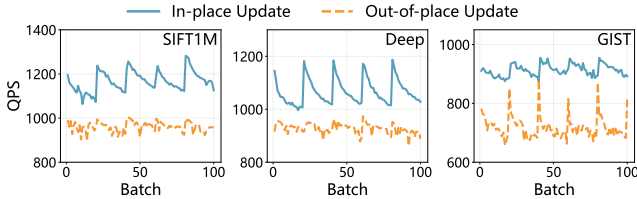


Figure 15: Search QPS under concurrent updates.

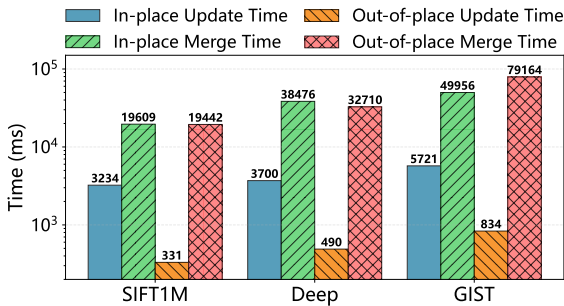


Figure 16: Average update and merge time (The merge time for in-place updates is consumed by the batch removal of nodes from the deletion queue).

4.3.5 *Update Efficiency.* We evaluate in-place (OdinANN) and out-of-place (FreshDiskANN) updates by executing 200K operations on an 800K-vector initial index. As shown in Figure 15, the in-place strategy consistently achieves higher sustained search throughput,

outperforming the out-of-place strategy by approximately 1.22×, 1.15×, and 1.27× on SIFT1M, Deep, and GIST, respectively. Figure 16 compares update latency and merge time across strategies. The out-of-place strategy consistently achieves lower update latency than in-place. On SIFT1M, Deep, and GIST, out-of-place update latency is 9.7×, 7.5×, and 6.8× lower than in-place, respectively, and its merge times are 0.99×, 0.85×, and 1.58× those of the in-place.

Findings: The in-place update favors query-heavy workloads by sustaining higher QPS, whereas the out-of-place update better suits update-heavy or balanced workloads due to its lower update latency.

5 LESSONS LEARNED

5.1 Technique Selection

Based on the experimental analysis, we summarize a decision tree (Figure 17) to guide technique selection across five key dimensions. **(1) Storage:** Under memory-constrained settings, we estimate the total memory footprint as

$$M_{\text{total}} = M_{\text{nav}} + M_{\text{pq}} + M_{\text{cache}} + C, \quad (1)$$

where the three major components are defined as

$$\begin{aligned}
 M_{\text{nav}} &= (d s_d + (1 + R) s_i) N, \\
 M_{\text{pq}} &= d s_d \cdot 2^{8k} + n_{\text{pq}} k N, \\
 M_{\text{cache}} &= M_{\text{dynamic}} + N_{\text{hot}} (d s_d + (1 + R) s_i).
 \end{aligned} \tag{2}$$

Here, M_{nav} , M_{pq} , and M_{cache} denote the memory footprints of the navigation graph, PQ structures, and caching layer, respectively. N is the number of vectors and N_{hot} the number of cached hot vectors. R denotes the maximum out-degree. d is the vector dimensionality; s_d and s_i represent the byte sizes of the vector data type and vector identifier (typically uint32). k (typically 1 byte) is the PQ code size per chunk and n_{pq} is the number of PQ chunks. M_{dynamic} denotes dynamically allocated cache space, and C captures working memory and auxiliary structures (typically below 50MB). Given a memory budget B , if $M_{\text{total}} \leq B$, we adopt the *major-in-disk* strategy; otherwise, we switch to the *all-in-disk* strategy.

(2) **Layout:** The disk layout strategy is primarily determined by vector dimensionality, as it directly affects block utilization and I/O efficiency. For low-dimensional data (typically $d \leq 1500$), we adopt *coupled global layout*; for high-dimensional data, *decoupled global layout* is preferred. For local layout, we use the *heuristic-based* strategy as a practical baseline, while more advanced designs remain an open direction (Section 5.2).

(3) **Caching:** The caching strategy is determined by vector dimensionality. For low-dimensional data (typically $d \leq 900$), *dynamic* or *hybrid* caching is preferred. For high-dimensional data, *static* (graph-prioritized) caching is recommended.

(4) **Query Execution:** The execution strategy is determined by the block packing factor (BPF), typically defined in conventional page layout structures (e.g., Starling), which measures how many vectors can be stored in a single disk page:

$$\text{BPF} = \frac{\text{page_size}}{d s_d + (1 + R) s_i}. \tag{3}$$

Based on BPF, the strategy is as follows. When $\text{BPF} < 2$, a disk page contains at most one vector on average, making I/O the dominant cost. In this case, we adopt an *I/O-driven* strategy with I/O–compute overlapping to mitigate access latency. When $\text{BPF} \geq 2$, multiple vectors can be amortized per page access, and computation becomes the dominant factor; thus, a *compute-driven* strategy is preferred.

(5) **Update:** The update technique is based on read–write ratio. For balanced or read-heavy workloads, in-place update technique is preferred. For write-heavy workloads, out-of-place is recommended.

5.2 Further Directions

Based on our findings and analysis, several open problems and research challenges remain in disk-resident graph-based ANN search.

(1) **Adaptive Design under Varying Dimensionality.** We observe that several methods exhibit markedly different performance as dimensionality increases, primarily due to degraded block locality and the higher cost of retrieving raw vectors. This sensitivity underscores the need for *dimension-aware design choices* and specialized mechanisms tailored to extreme high-dimensional settings, which remains an important direction for future research.

(2) **More Effective Layouts for Higher I/O Utilization.** Our results show that overall I/O utilization remains notably low across

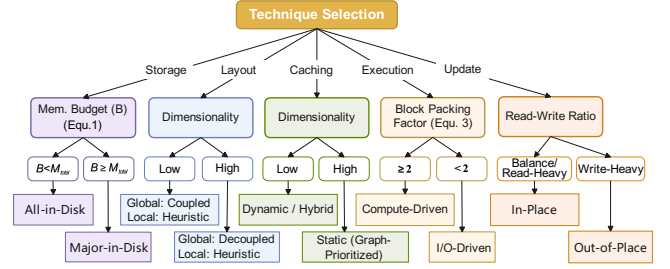


Figure 17: Technique Selection.

existing methods, primarily because current layout fail to colocate consecutive nodes along a search path into the same disk page. This motivates the design of more effective layout strategies that explicitly consider locality in graph traversals and the corresponding access patterns. Future directions include exploring traversal-aware or workload-adaptive layouts that dynamically reorganize disk blocks to enhance spatial locality and raise effective utilization.

(3) **More Efficient All-in-Disk Designs.** While all-in-disk designs offer attractive memory efficiency, our results show they generally lag behind major-in-disk methods in query performance. This gap is largely due to frequent disk accesses and limited opportunities for I/O–compute overlap. Designing more efficient all-in-disk methods that can better exploit locality, caching, and asynchronous execution, while preserving their low memory footprint, remains an important and open research direction.

(4) **Parameter Tuning under System and Workload Diversity.** The performance of disk-resident ANN systems is highly sensitive to a set of parameters, such as page size and beam width. Our findings indicate that changes in dimensionality can trigger stepwise performance degradation due to page-size shifts, while different execution strategies favor different parameter settings. Automatically tuning these parameters under varying datasets, dimensionalities, and hardware configurations remains an open challenge.

(5) **Extension to Cloud-Native Multi-Layer Storage.** Most existing disk-resident ANN systems are designed for heterogeneous memory-disk storage. However, modern cloud environments increasingly adopt multi-layer storage hierarchies, including memory, local SSD, and object storage. Extending disk-resident ANN designs to cloud-native, multi-layer storage settings raises new challenges in data placement, caching, and execution scheduling, especially under variable latency and bandwidth constraints.

6 CONCLUSION

In this paper, we systematically analyse disk-resident graph-based ANN methods across storage, layout, caching, query execution, and update mechanisms. Extensive evaluations are conducted to assess the performance of various methods across these five technical components. By analyzing the underlying trade-offs, we investigate the root causes of efficiency variations and summarize a wide range of meaningful findings. Based on our findings, we propose a comprehensive decision guide (Figure 17) structured around these five key components to clarify the best-fit designs for the scalable ANN search and suggest several promising avenues for future research.

REFERENCES

- [1] Laurent Amsaleg and Hervé Jégou. 2010. Datasets for approximate nearest neighbor search. <http://corpus-textmex.irisa.fr/>.
- [2] Karima Echihabi, Kostas Zoumpatianos, Themis Palpanas, and Houda Benbrahim. 2019. Return of the Lernaean Hydra: Experimental Evaluation of Data Series Approximate Similarity Search. *PVLDB* 13, 3 (2019), 403–420.
- [3] Elastic. 2023. kNN Search and Vector Fields in Elasticsearch. <https://www.elastic.co/guide/en/elasticsearch/reference/current/knn-search.html>. Accessed: 2025-12.
- [4] Charles Elkan. 2003. Using the triangle inequality to accelerate k-means. In *ICML*, Vol. 3. 147–153.
- [5] Cong Fu, Changxu Wang, and Deng Cai. 2021. High dimensional similarity search with satellite system graph: Efficiency, scalability, and unindexed query compatibility. *IEEE TPAMI* 44, 8 (2021), 4139–4150.
- [6] Cong Fu, Chao Xiang, Changxu Wang, and Deng Cai. 2019. Fast approximate nearest neighbor search with the navigating spreading-out graph. *PVLDB* 12, 5 (2019), 416–474.
- [7] GQR. 2018. GQR FVECS. <https://www.cse.cuhk.edu.hk/systems/hash/gqr/datasets.html>.
- [8] Hao Guo and Youyou Lu. 2025. Achieving Low-Latency Graph-Based Vector Search via Aligning Best-First Search Algorithm with SSD. In *OSDI*. 171–186.
- [9] Hao Guo and Youyou Lu. 2026. ODINANN: Direct Insert for Consistently Stable Performance in Billion-Scale Graph-Based Vector Search. *FAST* (2026).
- [10] Chengying Huan, Lizheng Chen, Zhengyi Yang, Shaonan Ma, Rong Gu, Renjie Yao, Zhibin Wang, Mingxing Zhang, Fang Xi, Jie Tao, et al. 2026. I/O Optimizations for Graph-Based Disk-Resident Approximate Nearest Neighbor Search: A Design Space Exploration. *arXiv preprint arXiv:2602.21514* (2026).
- [11] Cal Huang. 2025. *Migrating from S3 Vectors to Zilliz Cloud: Unlocking the Power of Tiered Storage*. <https://zilliz.com/blog/migrating-from-s3-vectors-to-zilliz-cloud-unlocking-the-power-of-tiered-storage> Blog post, Zilliz.
- [12] Turbopuffer Inc. 2025. *Turbopuffer — Serverless Vector & Full-Text Search Built from First Principles on Object Storage*. <https://turbopuffer.com/> Company website / product page.
- [13] Suhas Jayaram Subramanya, Fnu Devvrit, Harsha Vardhan Simhadri, Ravishankar Krishnawamy, and Rohan Kadekodi. 2019. Diskann: Fast accurate billion-point nearest neighbor search on a single node. *NeurIPS* 32 (2019).
- [14] Hervé Jégou, Matthijs Douze, and Cordelia Schmid. 2010. Product quantization for nearest neighbor search. *TPAMI* 33, 1 (2010), 117–128.
- [15] Dingyi Kang, Dongming Jiang, Hanshen Yang, Hang Liu, and Bingzhe Li. 2025. Scalable Disk-Based Approximate Nearest Neighbor Search with Page-Aligned Graph. *arXiv preprint arXiv:2509.25487* (2025).
- [16] Huiling Li and Jianliang Xu. 2025. BAMG: A Block-Aware Monotonic Graph Index for Disk-Based Approximate Nearest Neighbor Search. *arXiv preprint arXiv:2509.03226* (2025).
- [17] Mocheng Li, Xiao Yan, Baotong Lu, Yue Zhang, James Cheng, and Chenhao Ma. 2025. Attribute Filtering in Approximate Nearest Neighbor Search: An In-depth Experimental Study. *ACM SIGMOD* 3, 6 (2025), 1–26.
- [18] Wen Li, Ying Zhang, Yifang Sun, Wei Wang, Mingjie Li, Wenjie Zhang, and Xuemin Lin. 2019. Approximate nearest neighbor search on high dimensional data—experiments, analyses, and improvement. *IEEE TKDE* 32, 8 (2019), 1475–1488.
- [19] S. Lloyd. 1982. Least squares quantization in PCM. *IEEE Transactions on Information Theory* 28, 2 (1982), 129–137. <https://doi.org/10.1109/TIT.1982.1056489>
- [20] Jiahao Lou, Quan Yu, Shufeng Gong, Song Yu, Yanfeng Zhang, and Ge Yu. 2025. DGAI: Decoupled On-Disk Graph-Based ANN Index for Efficient Updates and Queries. *arXiv preprint arXiv:2510.25401* (2025).
- [21] Yury Malkov, Alexander Ponomarenko, Andrey Logvinov, and Vladimir Krylov. 2014. Approximate nearest neighbor algorithm based on navigable small world graphs. *Information Systems* 45 (2014), 61–68.
- [22] Yu A Malkov and Dmitry A Yashunin. 2018. Efficient and robust approximate nearest neighbor search using hierarchical navigable small world graphs. *IEEE TPAMI* 42, 4 (2018), 824–836.
- [23] Dingheng Mo, Junfeng Liu, Fan Wang, and Siqiang Luo. 2025. Aster: Enhancing LSM-structures for Scalable Graph Database. *ACM SIGMOD* 3, 1 (2025), 1–26.
- [24] Jionggang Ni, Xiaoliang Xu, Yuxiang Wang, Can Li, Jiajie Yao, Shihai Xiao, and Xuecang Zhang. 2023. DiskANN++: Efficient page-based search over isomorphic mapped graph index using query-sensitivity entry vertex. *arXiv preprint arXiv:2310.00402* (2023).
- [25] Yu Pan, Jianxin Sun, and Hongfeng Yu. 2023. Lm-diskann: Low memory footprint in disk-native dynamic graph-based ann indexing. *2023 IEEE International Conference on Big Data (BigData)* (2023), 5987–5996.
- [26] Yun Peng, Byron Choi, Tsz Nam Chan, Jianye Yang, and Jianliang Xu. 2023. Efficient Approximate Nearest Neighbor Search in Multi-dimensional Databases. *ACM SIGMOD* 1, 1 (2023), 1–27.
- [27] pgvector authors. 2023. pgvector: Open-source vector similarity search for Postgres. <https://github.com/pgvector/pgvector>. Accessed: 2025-12.
- [28] Qdrant. 2024. DBpedia Entities with OpenAI Embeddings (1M). <https://huggingface.co/datasets/Qdrant/dbpedia-entities-openai3-text-embedding-3-large-3072-1M>.
- [29] Aditi Singh, Suhas Jayaram Subramanya, Ravishankar Krishnaswamy, and Harsha Vardhan Simhadri. 2021. Freshdiskann: A fast and accurate graph-based ann index for streaming similarity search. *arXiv preprint arXiv:2105.09613* (2021).
- [30] Yitong Song, Pengcheng Zhang, Chao Gao, Bin Yao, Kai Wang, Zongyuan Wu, and Lin Qu. 2025. TRIM: Accelerating High-Dimensional Vector Similarity Search with Enhanced Triangle-Inequality-Based Pruning. *ACM SIGMOD* (2025).
- [31] Ji Sun, Guoliang Li, James Pan, Jiang Wang, Yongqing Xie, Ruicheng Liu, and Wen Nie. 2025. GaussDB-Vector: A Large-Scale Persistent Real-Time Vector Database for LLM Applications. *PVLDB* 18, 12 (2025), 4951–4963.
- [32] Kento Tatsuno, Daisuke Miyashita, Taiga Ikeda, Kiyoshi Ishiyama, Kazunari Sumiyoshi, and Jun Deguchi. 2024. AISAQ: All-in-Storage ANNS with Product Quantization for DRAM-free Information Retrieval. *arXiv preprint arXiv:2404.06004* (2024).
- [33] Yao Tian, Ziyang Yue, Ruiyuan Zhang, Xi Zhao, Bolong Zheng, and Xiaofang Zhou. 2023. Approximate Nearest Neighbor Search in High Dimensional Vector Databases: Current Research and Future Directions. *IEEE Data Eng. Bull.* 3 (2023), 39–54.
- [34] Jianguo Wang, Xiaomeng Yi, Rentong Guo, Hai Jin, Peng Xu, Shengjun Li, Xiangyu Wang, Xiangzhou Guo, Chengming Li, Xiaohai Xu, et al. 2021. Milvus: A purpose-built vector data management system. *ACM SIGMOD* (2021), 2614–2627.
- [35] Mengzhao Wang, Weizhi Xu, Xiaomeng Yi, Songlin Wu, Zhangyang Peng, Xiangyu Ke, Yunjun Gao, Xiaoliang Xu, Rentong Guo, and Charles Xie. 2024. Starling: An I/O-efficient disk-resident graph index framework for high-dimensional vector similarity search on data segment. *ACM SIGMOD* 2, 1 (2024), 1–27.
- [36] Mengzhao Wang, Xiaoliang Xu, Qiang Yue, and Yuxiang Wang. 2021. A comprehensive survey and experimental comparison of graph-based approximate nearest neighbor search. *arXiv preprint arXiv:2101.12631* (2021).
- [37] Yichuan Wang, Shu Liu, Zhifei Li, Yongji Wu, Ziming Mao, Yilong Zhao, Xiao Yan, Zhiying Xu, Yang Zhou, Ion Stoica, et al. 2025. LEANN: A Low-Storage Vector Index. *arXiv preprint arXiv:2506.08276* (2025).
- [38] Peiqi Yin, Xiao Yan, Qihui Zhou, Hui Li, Xiaolu Li, Lin Zhang, Meiling Wang, Xin Yao, and James Cheng. 2025. Gorgeous: Revisiting the Data Layout for Disk-Resident High-Dimensional Vector Search. *arXiv preprint arXiv:2508.15290* (2025).
- [39] Ziyang Yue, Bolong Zheng, Ling Xu, Kanru Xu, Shuhao Zhang, Yajuan Du, Yunjun Gao, Xiaofang Zhou, and Christian S Jensen. 2025. Select Edges Wisely: Monotonic Path Aware Graph Layout Optimization for Disk-Based ANN Search. *PVLDB* 18, 11 (2025), 4337–4349.
- [40] Cheng Zhang, Jianzhi Wang, Wan-Lei Zhao, and Shihai Xiao. 2025. Highly Efficient Disk-based Nearest Neighbor Search on Extended Neighborhood Graph. *ACM SIGIR* (2025), 2513–2523.
- [41] Xi Zhao, Yao Tian, Kai Huang, Bolong Zheng, and Xiaofang Zhou. 2023. Towards Efficient Index Construction and Approximate Nearest Neighbor Search in High-Dimensional Spaces. *PVLDB* 16, 8 (2023), 1979–1991.
- [42] Shurui Zhong, Dingheng Mo, and Siqiang Luo. 2025. LSM-VEC: A Large-Scale Disk-Based System for Dynamic Vector Search. *arXiv preprint arXiv:2505.17152* (2025).
- [43] Yijie Zhou, Shengyuan Lin, Shufeng Gong, Song Yu, Shuhao Fan, Yanfeng Zhang, and Ge Yu. 2025. GoVector: An I/O-Efficient Caching Strategy for High-Dimensional Vector Nearest Neighbor Search. *arXiv preprint arXiv:2508.15694* (2025).